Evaluating Seasonal Predictability of Antarctic Sea Ice and the importance of initial conditions with fully coupled models

Elio Campitelli[1,2*], Ariaan Purich[1,2], Julie Arblaster[1,2], Eun-Pa Lim[3], Mathew Wheeler[3], Phillip Reid[3]

[1]School of Earth, Atmosphere and Environment, Monash University, Australia,.

[2]Securing Antarctica's Environmental Future, Monash University, Australia.

[3]Research, Bureau of Meteorology.

*Corresponding author(s). E-mail(s): elio.campitelli@monash.edu;

Abstract

Accurate Antarctic sea-ice forecasts are crucial for climate monitoring and operational planning, yet they remain challenging due to model biases and complex ice-ocean-atmosphere interactions. We investigate the role of initial conditions on Antarctic sea-ice forecasts by comparing hindcasts from two versions of the Australian Bureau of Meteorology's ACCESS seasonal forecast system: ACCESS-S1 and ACCESS-S2. They use identical model configuration and differ only in their initial conditions; primarily in that ACCESS-S2 does not assimilate sea-ice observations. Our analysis reveals that both systems experience an extended melt season and delayed growth phase. This leads to a significant negative sea-ice extent bias which is corrected only in ACCESS-S1 by the data assimilation system. The impact of the initial conditions on forecast errors varies dramatically by season: summer and autumn initial conditions (January-April) provide predictive skill for up to three months, with February initial conditions being particularly crucial.

In contrast, winter forecasts off the two systems are statistically indistinguishable after only two weeks. Regional analysis of forecast skill suggests that this winter predictability barrier is most dramatic over Eastern Antarctica, where evern ACCESS-S1 shows negative skill. These findings highlight the critical importance of comprehensive year-round sampling in predictability studies and suggest that operational sea-ice data assimilation efforts should prioritize the summer-autumn period when initial conditions have maximum impact on forecast skill.

Keywords: sea ice, predictabilty, initial conditions, forecasting

Introduction

Accurately modelling Antarctic sea ice is essential for understanding processes and improving climate projections to inform adaptation strategies. Accurate seasonal to sub-seasonal forecasts are also crucial for operation contingency planning in and around the Antarctic continent, including scientific missions, fisheries, and tourism[1;2]. Improvements in modelled sea-ice might also help improve weather forecasts over and away from sea-ice regions[3–5].

However, producing accurate Antarctic sea-ice forecasts has been challenging due to model biases, inherent large variability and complexity, and they have lagged behind Arctic sea-ice forecasts[6;7]. Dynamical seasonal forecasts of summer Antarctic sea ice have been shown to perform worse than relatively simple statistical methods[8] and machine learning approaches e.g.[9;10], which also underscores the need for better understanding of sea-ice dynamics, and drivers of its variability.

Good initial conditions are generally required for a good forecast, however, it is not entirely known to what extent accurate sea-ice initial conditions affect the quality of the forecast and at what timescales. Exploring seasonal predictions of Arctic sea-ice, Guemas et al.[11] found that sea-ice initial conditions are important in autumn to predict summer sea-ice, but the impact wasn't as dramatic when predicting winter sea-ice. Day

et al.[12] also found seasonally-varying differences in the effect of initialisation, noting that accurate Arctic sea-ice thickness lead to improved sea-ice forecasts initialised in July but not when initialised in January.

For the Antarctic, Holland et al.[13] studied the initial-value predictability of Antarctic sea-ice in a perfect model study using the CCSM3 model. They found that sea-ice and ocean initial conditions provide predictive information to forecast sea-ice edge location several months in advance and that some predictability is retained for up to two years thanks to ocean heat content anomalies that are advected eastward. This is in contrast with Marchi et al.[14], who ran perfect model experiments to argue that uncertainty in the predicted atmospheric state and evolution is the main driver of uncertainty in Antarctic sea-ice extent prediction on seasonal timescales, with sea-ice and ocean initial conditions having lesser importance. More recently, Morioka et al.[15] studied decadal forecasts of Antarctic sea-ice and found that initialising ocean and sea-ice improved the correlation between simulated and observed sea-ice concentration evolution in the Amundsen–Bellingshausen Sea. It is hard to compare these studies since they are based on forecasts initialised at different times of the year and different frameworks: Holland et al.[13] ran 20 ensemble members initialised on the 1st of January of a particular year, Marchi et al.[14] ran forecasts from the 1st of March and 1st of September and Morioka et al.[15] run forecasts only from the 1st of March. Marchi et al.[14] also used a coupled ocean–sea-ice model instead of a fully coupled model like Holland et al.[13] did. Morioka et al.[15] used observed sea ice initial conditions and compared with observations, while Marchi et al.[14] and Holland et al.[13] are perfect model studies.

In October 2021 the Australian Bureau of Meteorology (BoM) upgraded the Australian Community Climate and Earth System Simulator – Seasonal (ACCES-S) from version S1 to S2. While the base model remained the same, the change in version was focused on using ocean, sea-ice and land initial conditions generated by the BoM instead of depending on the UK Met Office. Crucially, compared to ACCESS-S1, ACCESS-S2

does not assimilate sea-ice observations, so sea ice is only affected by the ocean and atmospheric data assimilation via the coupled integration.

Since model configuration is identical between ACCESS-S1 and ACCESS-S2, they form a sort of "natural experiment" where the same forecasting model was run over a long period of time with multiple ensemble forecasts initialised throughout the year, with the only difference being the initial conditions. This provides an opportunity to test the effect of sea-ice initial conditions on the forecast of sea-ice concentrations and the climate.

In this study we compare sea-ice hindcasts produced by ACCESS-S1 and ACCESS-S2. We focus on seasonality of errors and biases and the effect of the data assimilation system. This comparison will also inform future work with the prediction system as a research tool to better understand the dynamics and variability of the Antarctic sea ice and its impacts on the climate system as well as to explore the potential of using its sea-ice forecasts for decision-making. The work will also serve as a benchmark for future prediction systems to attempt to improve upon.

Data and methods

ACCESS-S2

ACCESS-S2[16] is the Bureau of Meteorology's seasonal forecast system which became operational in October 2021, replacing the ACCESS-S1 system[17]. The model components of both ACCESS-S2 and ACCESS-S1 are identical with the same numbers of levels and resolution. They consist of the Global Atmosphere 6.0 (GA6)[18;19], the Unified Model's Global Land 6.0[19;20], NEMO Global Ocean 5.0[21;22] and Global Sea Ice 6.0 [CICE; Rae et al.[23]]. The atmosphere has a N216 horizontal resolution (~60 km in the mid-latitudes) with 85 vertical levels. The land model uses the same horizontal

grid as the atmosphere with four soil levels. The ocean component has a nominal horizontal resolution of 1/4º with 75 vertical levels. The sea-ice component, based on CICE version 4.1, has the same resolution as the ocean component and five sea-ice thickness categories as well as an open water category.

Both systems take atmospheric initial conditions derived from ERA-interim[24] for their hindcasts. The main difference between the hindcasts of the two systems are the ocean and sea-ice initial conditions. ACCESS-S1 ocean initial conditions come from the Met Office FOAM system, which uses a multivariate, incremental three-dimensional variational (3D-Var), first-guess-at-appropriate-time (FGAT) data assimilation scheme[25] and assimilates sea surface temperature (SST), sea surface height (SSH), in situ temperature and salinity profiles, and sea-ice concentration. ACCESS-S2, on the other hand, is initialised from ocean conditions generated by the BoM weakly coupled ensemble data assimilation scheme described in Wedd et al.[16]. This scheme uses an optimal interpolation method and assimilates temperature and salinity profiles from EN4[26]. SSTs are nudged to Reynolds OISSTv2.1[27] in areas where SSTs are over 0ºC and Sea Surface Salinity is weakly nudged to the World Ocean Atlas 2013 climatology[28].

Of most relevance for this work, sea-ice concentrations are not assimilated in ACCESS-S2. Assimilation cycles are performed daily. The coupled model runs for 24 hours initialised from the previous cycle. Then the restart file fields of the ocean component are used as first guess in the data assimilation cycle and the innovations are used to build the next ocean initial conditions for the following cycle. The atmosphere fields from that daily integration are not used and instead the model atmosphere is initialised using ERA-Interim. The sea-ice initial conditions for the next cycle are the unaltered output of the previous daily integration. Then the cycle starts again and the coupled model runs for another 24 hours. During this integration the sea-ice component is affected by the ocean innovations and the new atmosphere initial conditions via the coupler.

The ACCESS-S2 hindcast set used in this study runs for the period 1981–2018. Each hindcast consists of nine ensemble members built from three consecutive 3-member forecasts initialised at the first of every month and the two previous days and run for 279 days. The ACCESS-S1 hindcast set is built by perturbing the atmospheric fields only with a random field perturbation[17] and runs for 217 days for the period 1990–2012. We analise the ensemble mean hindcasts unless otherwise specified.

Anomalies for each hindcast set are taken with respect to their own climatology specific to each initialisation date and forecast lead time, for the period 1990–2012. This serves as a first-order correction of model bias and drift.

Besides sea-ice concentration, we also analyse mean sea-ice thickness, which we compute as total sea-ice volume divided by total sea-ice area.

Verification datasets

For verification we use satellite-derived sea-ice concentration, which estimates the proportion of each grid area that is covered with ice. Datasets derived using different algorithms and satellite platforms, each have their own biases and uncertainties. Estimates of inter-product uncertainty of sea-ice extent (SIE, defined here as the total region of the Southern Ocean with at least 15% sea-ice cover) is of the order of 0.5 million km^2 [29]. As will be shown below, this spread is minimal compared with the typical errors in the ACCESS-S2 and ACCESS-S1 forecasts, so the overall conclusions of this study are independent of the verification dataset used.

We use NOAA/NSIDC's Climate Data Record V4 [CDR; Meier et al.[30]] as the primary sea-ice verification dataset. It takes the maximum value of the NASA Team[31] and NASA Bootstrap[32] sea-ice concentration products to reduce their low concentration bias[30;33]. Both source algorithms use data from the Scanning Multichannel Microwave Radiometer (SMMR) on the Nimbus-7 satellite and from the Special Sensor

Microwave/Imager (SSM/I) sensors on the Defense Meteorological Satellite Program's (DMSP) -F8, -F11, and -F13 satellites. The data has a spatial resolution of 25 by 25 km and daily from 1978 onwards.

The European Organisation for the Exploitation of Meteorological Satellites (EUMETSAT) Ocean and Sea Ice Satellite Application Facility[34] based on the SSMIS sensor is another satellite-derived sea-ice concentration product. It is based on mostly the same sensors as the NOAA CDR but computed independently using different algorithms. Figures prepared with this dataset are provided in the supplementary material and do not differ significantly from the ones prepared using CDR.

Error measures

For evaluation purposes, we use a series of measures.

Sea-ice extent is defined as the area of the ocean at least 15% covered by sea-ice. This threshold is motivated by the limitations in satellite retrieval, which is increasingly unreliable for lower sea-ice concentrations[35].

Pan-Antarctic (net) sea-ice extent serves as a hemispheric measure of the amount of sea ice, but it does not take into account the spatial distribution. A model could have a relatively accurate extent of the net ice but with different regional distributions. To account for location errors, we computed the Root Mean Squared Error (RMSE) of grid-point sea-ice concentration anomalies.

We compute RMSE as the square root of the area-averaged squared differences between grid-point forecasted and observed sea-ice concentration anomalies. We compute a pan-Antarctic RMSE by averaging over the whole NOAA/NSIDC CDRV4 Southern Hemisphere domain, and also a zonally-varying RMSE computed over twenty-four 15° longitude slices around Antarctica.

All error measures were computed on the NOAA/NSIDC CDRV4 domain grid, to which model output was bilinearly interpolated. Note that the ACCESS CICE model grid has resolution between two and three times higher than NOAA/NSIDC CDRV4.

Forecasts errors are also compared with hypothetical forecasts based on the persistence of anomalies and on climatology. The persistence forecast is generated by extending the observed anomalies in time.

As a measure of forecast improvement over the hypothetical forecast, we use the skill score[36], defined as

$$S = 1 - \frac{RMSE_f}{RMSE_r}$$

Where $RMSE_f$ is the RMSE of the forecast, $RMSE_r$ is the RMSE of the reference forecast. Negative skill score indicates that the forecast is worse than the reference forecast while positive values indicate an improvement. A perfect forecast, would have zero RMSE and thus a skill score of 1.

Results and discussion

Bias

Figure 1 shows the mean sea-ice extent of the ACCESS-S2 and ACCESS-S1 hindcasts (row a) and their differences from the mean sea-ice extent of NOAA/NSIDC CDRV4 (row b). Mean extent at the first of every month is indicated with circles for the initial conditions and with triangles for the longest lead time possible for each model (between 274 and 277 days for ACCESS-S2 and between 213 and 216 days for ACCESS-S1). At this long lead time, the information of the initial conditions is essentially lost and the forecast reverts to each model's preferred equilibrium state.

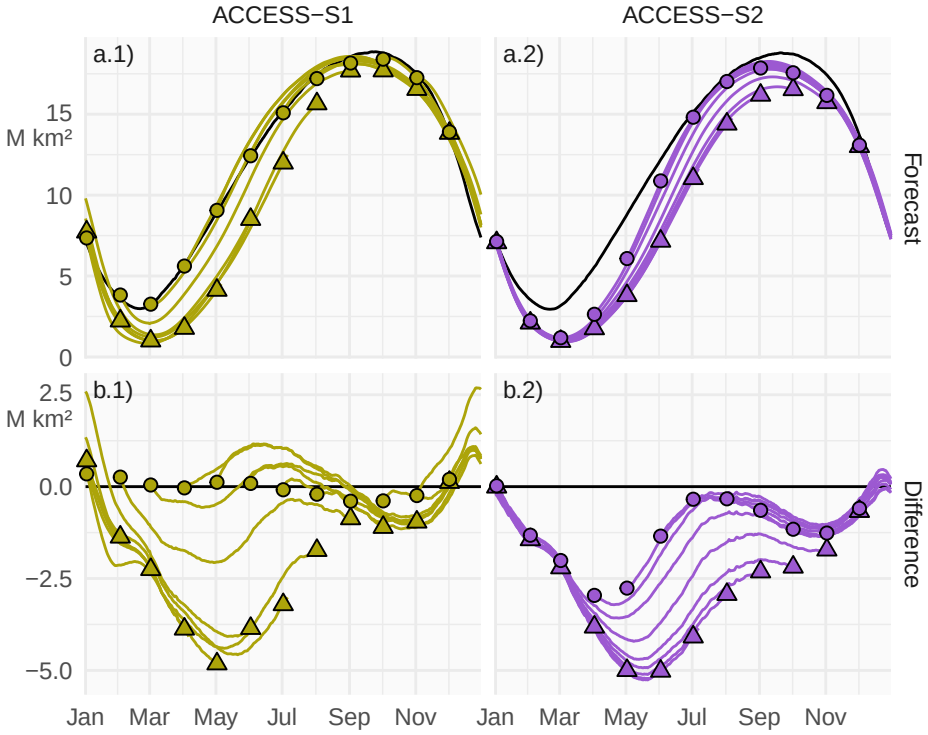

Figure 1: Row a: Pan-Antarctic mean sea-ice extent for all hindcasts initialised on the first of each calendar month for ACCESS-S1 (column 1; green) and ACCESS-S1 (column 2; purple). Mean sea-ice extent from NOAA/NSIDC CDRV4 in each corresponding hindcast period is shown in black. Row b: Mean differences between the forecast and the observed values. Circles represent the initial conditions at the start of forecasts (i.e., the first of every month), and triangles represent the mean values at the end of forecasts (i.e., the longest possible lead time).

ACCESS-S2 initial conditions (circles; Figure 1 column 1) show an overall negative bias, especially in the late summer-early autumn, while ACCESS-S1 initial conditions (circles in Figure 1 column 2) are very close to observations, as expected from the assimilation of sea-ice observations to produce the initial conditions of ACCESS-S1. Both systems' equilibrium states (triangles) show negative biases of sea-ice extent, particularly in the growth phase of late-autumn and winter months. This is due primarily to the melt season being longer than in observations and with faster melt between January and March and the growing seasons being shorter with slower growth during March and

April. This is then followed by faster growth between May and July (Figure 2). Many sea-ice models exhibit this systematic underestimation during the sea-ice minimum and early freezing season[8], which could indicate problems in the representation of thermodynamics in the model[6]. It is also not surprising that both forecasting systems converge to a similar equilibrium state because they share the same model formulation.

The difference between the initial conditions (circles) and the model equilibrium state (triangles) can be mostly attributed to the effect of data assimilation, which in ACCESS-S2 is due solely to atmospheric and oceanic data assimilation. From May to October, in ACCESS-S2 circles are closer to observations than to the triangles, indicating that the information from the ocean and atmosphere data assimilation is affecting sea ice and improving the initial conditions. During these months, ACCESS-S1 can overestimate the sea-ice extent at short lead time. For the rest of the year circles are overlaid with triangles in ACCESS-S2, indicating that the ocean and atmosphere data assimilation is not affecting sea ice and that this component of the model is virtually free-running.

To further understand the bias in ACCESS-S2, Figure 3 shows spatial patterns of the differences of monthly mean sea-ice concentrations between NOAA/NSIDC CDRV4 and ACCESS-S2 hindcasts at the shortest monthly lead time. From October to May, the model underestimates sea-ice concentrations in most regions except for the inner Weddell Sea in April and May, where sea-ice concentrations saturate to 1 both in the observations and forecasts. In winter, the differences are limited to a narrow band around the sea-ice edge with slight positive biases in the African sector of East Antarctica and negative biases around the Indian Ocean sector which partially compensate, resulting in the near-zero extent bias seen in those months (Figure 1).

ACCESS-S1 has a comparatively smaller overall bias (Figure 4). The largest values are found between April and June, when the faster growth resutls in large positive bias along the sea-ice edge, and in January, when the faster melt leads to large negative bias in the Weddell and Admunsen seas.

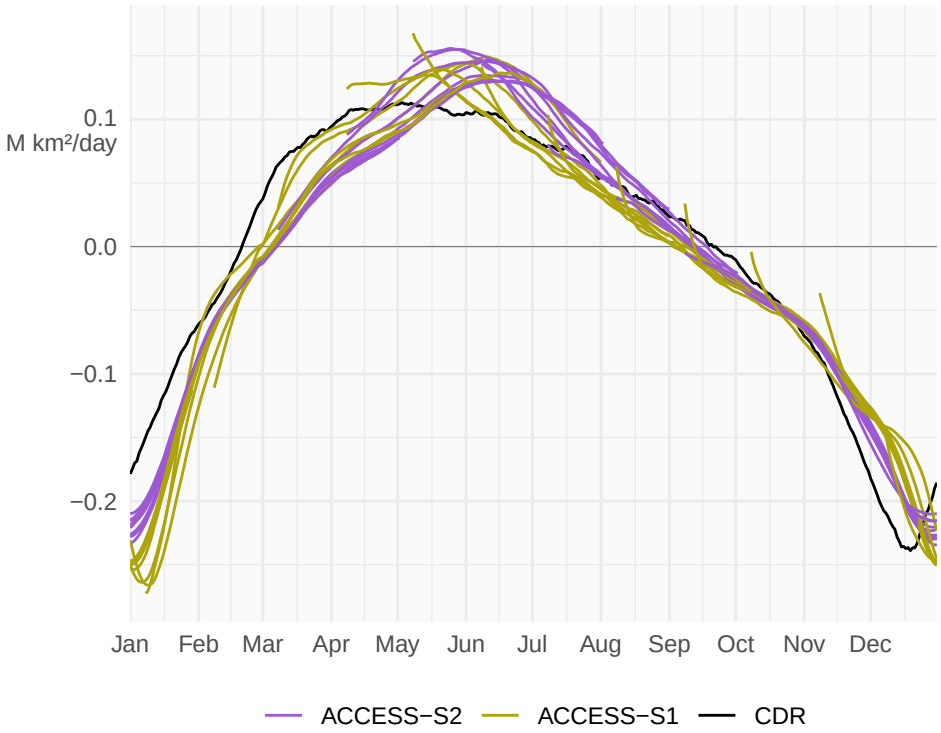

Figure 2: Mean daily sea-ice extent growth (10^6 km^2/day) in ACCESS-S1 (green) and ACCESS-S2 (purple) hindcasts and observations (black), computed as the mean daily differences in sea-ice extent between each date and the next for each forecast month. Values are smoothed with a 11-day running mean.

RMSE

Figure 5 shows monthly sea-ice extent anomalies forecasted at selected lead times. Compared with ACCESS-S1, ACCESS-S2 anomaly forecasts are relatively poor (large RMSE) even for the first month (lead time 0), whereas ACCESS-S1 forecasts stay relatively skilful even at a lead time of three months. ACCESS-S2 shows much larger interannual variability than observations, with dramatic lows between 1995 and 2007, and highs between 2007 and 2015.

Unexpectedly, for ACCESS-S2, RMSE improves with lead time, even though the correlation degrades with lead time. This is puzzling behaviour that goes contrary to

what is usually seen in prediction models. The explanation seems to be the mentioned increased interannual variability. Figure 6 shows monthly mean sea-ice extent of the forecasts as a function of lead time compared with observations. ACCESS-S1 standard deviation lies within the observed standard deviation regardless of lead time, while ACCESS-S2 standard deviation is more than twice that of observations at zero lead time and only approaches the observed value at 9 month lead time for most months.

ACCESS-S2 forecasts of sea-ice extent anomalies seem to align moderately well with observations (leading to moderately high correlation) but their magnitude is overestimated (leading to large errors). This could be caused by ACCESS-S2 sea ice being much more sensitive to atmospheric and oceanic forcing, perhaps due to lower thickness.

As an example, Figure 7 shows sea-ice concentration anomalies (top row) and sea-ice thickness and the difference between the two models (bottom row) for 2 May 2008 initialised one day prior; being that close to initialisation date, these are very approximately the initial conditions. ACCESS-S1 sea-ice concentrations anomalies are very close to observations as expected from the system assimilating these data. ACCESS-S2 sea-ice concentration anomalies, which are not assimilated, are not as close, but the large-scale pattern is aligned with observations. The system simulates large positive anomalies in the Weddell and Ross seas and slight negative anomalies in the Amundsen and Bellingshausen seas. The fact that ACCESS-S2 can simulate this pattern without assimilating sea-ice data suggests that atmospheric and oceanic forcing was the dominant factor. However, the magnitude of the sea-ice anomalies is too big. It is plausible that this is due to the thinner ice simulated by ACCESS-S2 (bottom row).

Extending beyond the one case in Figure 7, Figure 8 shows monthly mean sea-ice thickness as a function of lead time for ACCESS-S1 and ACCESS-S2. Supporting the idea that thinner ice is what causes the increased extent variability in ACCESS-S2, this system simulates thinner sea-ice compared to ACCESS-S1 overall at almost all lead times and in all months except for summer at short lead times (Dec-Jan, 0-1

months; Feb-Mar, 0-2 months). However, in both systems, forecasted sea-ice is thicker at shorter lead times and then decreases, particularly in the summer months. If thinner ice were a sufficient cause of increased variability, then we would expect variability to increase with lead time in both forecasting systems.

The fact that ACCESS-S1 and ACCESS-S2 share the same model configuration and that the increased variability is more extreme at short lead times (Fig. 6) suggests that the data assimilation procedure is partly to blame. It is possible that sea-ice in the ACCESS-S2 system is left in an unbalanced state after assimilating atmospheric and oceanic data but not sea-ice data, leading to large responses that are amplified by the thin ice in the initial states which then subside at longer lead times when the model is balanced.

To assess ACCESS-S2 forecasts in more detail, we compute error measures for all hindcasts started on the 1st of every month.

Figure 9 shows the mean RMSE of sea-ice concentration anomalies for ACCESS-S1 and ACCESS-S2 hindcasts compared against persistence and climatological forecasts used as a benchmark. Due to errors in the initial conditions, it is expected that persistence forecasts would be better than the model forecasts at very short lead times, but that the persistence forecast errors would grow faster and may eventually surpass the model forecast errors. The black line shows that the persistence forecast error indeed grows rapidly and reaches its maximum in about 30 days for most months except for February, when it grows much slower. The ACCESS-S1 forecast errors grow slower than persistence forecast errors and remain lower after less than 10 days on average. The ACCESS-S2 forecast error starts high in all months and is lower than the persistence forecast error after more than 15 days in most months except for forecast initialised in February, when it takes 80 days.

At longer lead times, it is more appropriate to compare errors with the climatological forecast error. The lead time at which ACCESS-S1 forecast error is higher than the climatological forecast error varies between more than 60 and less than 20 days depending on forecast initialisation month with the minimum in June. ACCESS-S2 forecasts never have lower error than climatology, on the other hand, except marginally in October forecasts.

Figure 10 summarises the lead time window in which each hindcast is better than both the persistence forecast and the climatological forecast as a function of forecast month. ACCESS-S1 forecasts have a wider lead time window in the summer than the other seasons and is not better than both benchmarks at forecasting June sea-ice concentration anomalies. Forecasts initialised in May and June are particularly poor, and July cannot be forecasted better than the benchmarks. This is consistent with the mid-winter loss of predictability observed by Libera et al.[37], who attributed it to deep warm water entraining into the mixed layer.

To analyse the spatial distribution of the model error, we computed the RMSE of zonal mean sea-ice concentration anomalies on 15 slices of `diff(unique(rmse_lon_mean$lon))[1]`° longitude span for each forecasting system. We control for some areas being naturally easier to forecast than others by computing the RMSE skill score with the climatological forecast RMSE as reference.

For ACCESS-S1 forecasts (Figure 11), skill tends to be lower off the coast of Eastern Antarctica even at short lead times; for instance, the skill score for forecasts initialised in May and June are negative between 0° and 120°E even at almost zero lead time. This mirrors Libera et al.[37] findings of a "winter predictability barrier", although they focus on the Weddell sea and here we show that the effect seems to be stronger more to the East. In western Antarctica there is a hint of easterly-propagating skill in forecasts initialised in February and March. This is consistent with Holland et al.[13]

findings that memory of sea-ice anomalies are stored in ocean heat content anomalies that are transported east by the Antarctic Circumpolar Current.

ACCESS-S2 forecasts (Figure 12) also have lower skill over Eastern Antarctica. From July to December even though the pan-Antarctic average skill is negative at all lead times (Fig. 10), it is positive for up to a month in Western Antarctica. Since oceanic and atmospheric forcing is the only source of information, this suggests that sea-ice in this region is particularly sensitive to oceanic and atmospheric forcing and suggests a role of the Pacific-South American mode and the Amundsen Sea Low to shape sea-ice concentration anomalies. The fact that this is evident in the months in which ENSO teleconnections are more important for atmospheric circulation also suggest the influence of tropical Pacific variability. February and March are the only two months that can be forecasted with marginally positive skill in large regions.

In Figure 5 the mean error was shown. Figure 13 column 1 shows the mean standard deviation of errors among ensemble members at various lead times. At one day lead time (Fig. 13 a.1) ACCESS-S2 has a slightly larger spread than ACCESS-S1 due to the way that ensemble members are generated. ACCESS-S1 ensemble members are generated by adding random field perturbations to the atmosphere only, which then are transferred to the other components via the coupled simulation[17]. With this scheme, ensemble members are all but guaranteed to be underdispersed in the ocean and sea-ice components. The time-lag ensemble used for ACCESS-S2 ensures greater spread. This difference is gone after about just two days, and both systems have a comparable spread in ensemble member error afterwards (Fig. 13 b1 and c1).

Figure 13 column 2, on the other hand, shows the standard deviation of ensemble mean error of each hindcast and the persistence forecast. At one day lead time, ACCESS-S2 ensemble mean error standard deviation is much larger than ACCESS-S1's, which in turn is comparable to the persistence forecast error standard deviation. At longer lead times, the spread of ACCESS-S1 and persistence forecast standard deviation increases

to eventually be comparable to ACCESS-S2 and the standard deviation in climatological forecast errors. ACCESS-S2 error standard deviation is fairly independent of lead time and similar to the climatological forecast error standard deviation at all lead times.

Conclusions

Sea-ice forecasts from the ACCESS-S2 system show a significant low extent bias, particularly during late summer and early autumn. This bias is attributed to a faster and longer melt season between January and March, and slower growth between March and April. This underestimation during the minimum and early freezing season is a common issue in many seasonal-to-subseasonal (S2S) systems, suggesting potential problems either with the model's thermodynamic representation or with short wave radiation forcing, as shown in other climate models[6;38]. Even though ACCESS-S2 shares the same model formulation with ACCESS-S1, the latter does not suffer from this bias, indicating that assimilating sea-ice concentrations successfully corrects for the negative bias that exists in the free-running model.

Ensemble spread grows quickly even when perturbations are only implemented in the atmosphere component (in ACCESS-S1), indicating that sea-ice is indeed responding quickly to atmospheric perturbations. However, our analysis suggests that the atmosphere and ocean data assimilation implemented in ACCESS-S2 is only effectively influencing sea-ice initial conditions from June to October, while the rest of the year, the sea-ice component runs virtually free, reverting to its biased equilibrium state.

Analysis of the error spread shows that ACCESS-S2 initial conditions from December to May not only have large errors, but that the initial error spread is very large compared with ACCESS-S1. This spread is not due to the perturbation scheme, since the mean error variance for individual forecasts is low and comparable with ACCESS-S1. Instead, it is due to large variance of the mean error of individual forecasts, which

is comparable to the climatology spread. This is further evidence that individual initial conditions are not being affected by the data assimilation scheme.

Although ACCESS-S1 only assimilates sea-ice concentration, it is clear that sea-ice thickness is also affected. ACCESS-S1 simulates significantly thicker ice than ACCESS-S2 and in both systems sea-ice is thicker at shorter lead times than at longer lead times. Both the explicit data assimilation in ACCESS-S2 and the effects of atmospheric and oceanic data assimilation in ACCESS-S1 might be nudging simulated sea ice to be thicker than the model equilimbrium state.
We believe that the thinner sea-ice in ACCESS-S2 is a partial cause for the large sea-ice extent variance, but other mechanisms, such as unbalanced initial conditions might be important.

Given that ACCESS-S2 sea-ice extent is essentially not initialised by the observations, comparing its forecasts with those of ACCESS-S1 allows us to estimate the time-scale for which initial conditions are important. We find that initial conditions affect Antarctic sea-ice forecasts in ther order of a few months, but that effect is seasonally dependent. January to April initial conditions improve forecasts for up to 3 months with, February initial conditions in particular are shown to be crucial for determining sea-ice evolution at least up to May. Arctic sea-ice forecasts also show greater sensitivity to initial conditions in boreal summer, compared with boreal winter[12;39], suggesting a similar mechanism might be playing a role.

Forecasts initialised in winter have very little skill and ACCESS-S1 and ACCESS-S2 forecast errors are not statistically different after just 2 weeks. This is consistent with Libera et al.[37]'s finding of a "winter predictability barrier" in the Weddell sea, although they describe the barrier as sharp loss of predictability in July, and here we find a gradual reduction in skill compared with climatology around June. This difference might be due to our use of pan-Antarctic RMSE, since our regional analysis indicates that the degraded skill is most dramatic in the King Haakon sea.

These findings have important implications for both operational forecasting, model development and predictability studies. For operational centers, our results suggest that efforts to improve sea-ice data assimilation should prioritize the summer and autumn months when initial conditions have the greatest impact on forecast skill. Additionally, the substantial bias in ACCESS-S2 highlights the need for improved model physics, particularly in the representation of sea-ice thermodynamics and radiation processes. Crucially, our results suggest dramatic seasonal variations in sea-ice predictability. Future studies should therefore use initial conditions through the whole year rather than focusing on a limited number of initialisation dates.

References

[1] De Silva, L.W.A., Inoue, J., Yamaguchi, H., Terui, T.: Medium range sea ice prediction in support of Japanese research vessel MIRAI's expedition cruise in 2018. Polar Geography **43**(2-3), 223–239 (2020) https://doi.org/10.1080/1088937X.2019.1707317 . Publisher: Taylor & Francis _eprint: https://doi.org/10.1080/1088937X.2019.1707317. Accessed 2024-10-17

[2] Wagner, P.M., Hughes, N., Bourbonnais, P., Stroeve, J., Rabenstein, L., Bhatt, U., Little, J., Wiggins, H., Fleming, A.: Sea-ice information and forecast needs for industry maritime stakeholders. Polar Geography **43**(2-3), 160–187 (2020) https://doi.org/10.1080/1088937X.2020.1766592 . Publisher: Taylor & Francis _eprint: https://doi.org/10.1080/1088937X.2020.1766592. Accessed 2024-10-07

[3] Rinke, A., Maslowski, W., Dethloff, K., Clement, J.: Influence of sea ice on the atmosphere: A study with an Arctic atmospheric regional climate model. Journal of Geophysical Research: Atmospheres **111**(D16) (2006) https://doi.

org/10.1029/2005JD006957 . _eprint: https://agupubs.onlinelibrary.wiley.com/-doi/pdf/10.1029/2005JD006957. Accessed 2025-08-05

[4] Wang, Z., Fraser, A.D., Reid, P., Coleman, R., O'Farrell, S.: The Influence of Time-Varying Sea Ice Concentration on Antarctic and Southern Ocean Numerical Weather Prediction. Weather and Forecasting **39**(2), 293–310 (2024) https://doi.org/10.1175/WAF-D-22-0220.1 . Publisher: American Meteorological Society Section: Weather and Forecasting. Accessed 2025-08-05

[5] Semmler, T., Kasper, M.A., Jung, T., Serrar, S.: Remote impact of the Antarctic atmosphere on the southern mid?latitudes. Meteorologische Zeitschrift **25**(1), 71–77 (2016) https://doi.org/10.1127/metz/2015/0685 . Place: Stuttgart, Germany Publisher: Schweizerbart Science Publishers

[6] Zampieri, L., Goessling, H.F., Jung, T.: Predictability of Antarctic Sea Ice Edge on Subseasonal Time Scales. Geophysical Research Letters **46**(16), 9719–9727 (2019) https://doi.org/10.1029/2019GL084096 . _eprint: https://onlinelibrary.wiley.com/doi/pdf/10.1029/2019GL084096. Accessed 2024-10-17

[7] Gao, Y., Xiu, Y., Nie, Y., Luo, H., Yang, Q., Zampieri, L., Lv, X., Uotila, P.: An Assessment of Subseasonal Prediction Skill of the Antarctic Sea Ice Edge. Journal of Geophysical Research: Oceans **129**(11), 2024–021499 (2024) https://doi.org/10.1029/2024JC021499 . _eprint: https://agupubs.onlinelibrary.wiley.com/-doi/pdf/10.1029/2024JC021499. Accessed 2025-07-30

[8] Massonnet, F., Barreira, S., Barthélemy, A., Bilbao, R., Blanchard-Wrigglesworth, E., Blockley, E., Bromwich, D.H., Bushuk, M., Dong, X., Goessling, H.F., Hobbs, W., Iovino, D., Lee, W.-S., Li, C., Meier, W.N., Merryfield, W.J., Moreno-Chamarro, E., Morioka, Y., Li, X., Niraula, B., Petty, A., Sanna, A., Scilingo, M., Shu, Q., Sigmond, M., Sun, N., Tietsche, S., Wu, X., Yang, Q., Yuan, X.:

SIPN South: six years of coordinated seasonal Antarctic sea ice predictions. Frontiers in Marine Science **10** (2023) https://doi.org/10.3389/fmars.2023.1148899 . Publisher: Frontiers. Accessed 2024-10-17

[9] Dong, X., Yang, Q., Nie, Y., Zampieri, L., Wang, J., Liu, J., Chen, D.: Antarctic sea ice prediction with A convolutional long short-term memory network. Ocean Modelling **190**, 102386 (2024) https://doi.org/10.1016/j.ocemod.2024.102386 . Accessed 2025-07-30

[10] Lin, Y., Yang, Q., Li, X., Dong, X., Luo, H., Nie, Y., Wang, J., Wang, Y., Min, C.: Ice-kNN-South: A Lightweight Machine Learning Model for Antarctic Sea Ice Prediction. Journal of Geophysical Research: Machine Learning and Computation **2**(1), 2024–000433 (2025) https://doi.org/10.1029/2024JH000433 . _eprint: https://agupubs.onlinelibrary.wiley.com/doi/pdf/10.1029/2024JH000433. Accessed 2025-07-30

[11] Guemas, V., Chevallier, M., Déqué, M., Bellprat, O., Doblas-Reyes, F.: Impact of sea ice initialization on sea ice and atmosphere prediction skill on seasonal timescales. Geophysical Research Letters **43**(8), 3889–3896 (2016) https://doi.org/10.1002/2015GL066626 . _eprint: https://agupubs.onlinelibrary.wiley.com/doi/pdf/10.1002/2015GL066626. Accessed 2025-07-30

[12] Day, J.J., Hawkins, E., Tietsche, S.: Will Arctic sea ice thickness initialization improve seasonal forecast skill? Geophysical Research Letters **41**(21), 7566–7575 (2014) https://doi.org/10.1002/2014GL061694 . _eprint: https://onlinelibrary.wiley.com/doi/pdf/10.1002/2014GL061694. Accessed 2024-08-16

[13] Holland, M.M., Blanchard-Wrigglesworth, E., Kay, J., Vavrus, S.: Initial-value predictability of Antarctic sea ice in the Community Climate System Model 3. Geophysical Research Letters **40**(10), 2121–2124 (2013) https://doi.org/10.1002/

grl.50410 . _eprint: https://onlinelibrary.wiley.com/doi/pdf/10.1002/grl.50410. Accessed 2024-12-10

[14] Marchi, S., Fichefet, T., Goosse, H.: Respective influences of perturbed atmospheric and ocean–sea ice initial conditions on the skill of seasonal Antarctic sea ice predictions: A study with NEMO3.6–LIM3. Ocean Modelling **148**, 101591 (2020) https://doi.org/10.1016/j.ocemod.2020.101591 . Accessed 2025-07-30

[15] Morioka, Y., Iovino, D., Cipollone, A., Masina, S., Behera, S.K.: Decadal Sea Ice Prediction in the West Antarctic Seas with Ocean and Sea Ice Initializations. Communications Earth & Environment **3**(1), 189 (2022) https://doi.org/10.1038/s43247-022-00529-z . Publisher: Nature Publishing Group. Accessed 2025-07-30

[16] Wedd, R., Alves, O., Burgh-Day, C.d., Down, C., Griffiths, M., Hendon, H.H., Hudson, D., Li, S., Lim, E.-P., Marshall, A.G., Shi, L., Smith, P., Smith, G., Spillman, C.M., Wang, G., Wheeler, M.C., Yan, H., Yin, Y., Young, G., Zhao, M., Xiao, Y., Zhou, X.: ACCESS-S2: the upgraded Bureau of Meteorology multi-week to seasonal prediction system. Journal of Southern Hemisphere Earth Systems Science **72**(3), 218–242 (2022) https://doi.org/10.1071/ES22026 . Publisher: CSIRO PUBLISHING. Accessed 2024-10-07

[17] Hudson, D., Alves, O., Hendon, H.H., Lim, E.-P., Liu, G., Luo, J.-J., MacLachlan, C., Marshall, A.G., Shi, L., Wang, G., Wedd, R., Young, G., Zhao, M., Zhou, X.: ACCESS-S1 The new Bureau of Meteorology multi-week to seasonal prediction system. Journal of Southern Hemisphere Earth Systems Science **67**(3), 132–159 (2017) https://doi.org/10.1071/es17009 . Publisher: CSIRO PUBLISHING. Accessed 2024-10-07

[18] Williams, K.D., Harris, C.M., Bodas-Salcedo, A., Camp, J., Comer, R.E., Copsey, D., Fereday, D., Graham, T., Hill, R., Hinton, T., Hyder, P., Ineson, S., Masato, G.,

Milton, S.F., Roberts, M.J., Rowell, D.P., Sanchez, C., Shelly, A., Sinha, B., Walters, D.N., West, A., Woollings, T., Xavier, P.K.: The Met Office Global Coupled model 2.0 (GC2) configuration. Geoscientific Model Development **8**(5), 1509–1524 (2015) https://doi.org/10.5194/gmd-8-1509-2015 . Publisher: Copernicus GmbH. Accessed 2024-10-11

[19] Waters, J., Bell, M.J., Martin, M.J., Lea, D.J.: Reducing ocean model imbalances in the equatorial region caused by data assimilation. Quarterly Journal of the Royal Meteorological Society **143**(702), 195–208 (2017) https://doi.org/10.1002/qj.2912 . _eprint: https://onlinelibrary.wiley.com/doi/pdf/10.1002/qj.2912. Accessed 2024-10-11

[20] Best, M.J., Pryor, M., Clark, D.B., Rooney, G.G., Essery, R.L.H., Ménard, C.B., Edwards, J.M., Hendry, M.A., Porson, A., Gedney, N., Mercado, L.M., Sitch, S., Blyth, E., Boucher, O., Cox, P.M., Grimmond, C.S.B., Harding, R.J.: The Joint UK Land Environment Simulator (JULES), model description – Part 1: Energy and water fluxes. Geoscientific Model Development **4**(3), 677–699 (2011) https://doi.org/10.5194/gmd-4-677-2011 . Publisher: Copernicus GmbH. Accessed 2024-10-11

[21] Gurvan, M., Bourdallé-Badie, R., Bouttier, P.-A., Bricaud, C., Bruciaferri, D., Calvert, D., Chanut, J., Clementi, E., Coward, A., Delrosso, D., Ethé, C., Flavoni, S., Graham, T., Harle, J., Iovino, D., Lea, D., Lévy, C., Lovato, T., Martin, N., Masson, S., Mocavero, S., Paul, J., Rousset, C., Storkey, D., Storto, A., Vancoppenolle, M.: NEMO ocean engine (2013) https://doi.org/10.5281/zenodo.1475234 . Publisher: Zenodo. Accessed 2024-10-11

[22] Megann, A., Storkey, D., Aksenov, Y., Alderson, S., Calvert, D., Graham, T., Hyder, P., Siddorn, J., Sinha, B.: GO5.0: the joint NERC–Met Office NEMO

global ocean model for use in coupled and forced applications. Geoscientific Model Development **7**(3), 1069–1092 (2014) https://doi.org/10.5194/gmd-7-1069-2014 . Publisher: Copernicus GmbH. Accessed 2024-10-11

[23] Rae, J.G.L., Hewitt, H.T., Keen, A.B., Ridley, J.K., West, A.E., Harris, C.M., Hunke, E.C., Walters, D.N.: Development of the Global Sea Ice 6.0 CICE configuration for the Met Office Global Coupled model. Geoscientific Model Development **8**(7), 2221–2230 (2015) https://doi.org/10.5194/gmd-8-2221-2015 . Publisher: Copernicus GmbH. Accessed 2024-10-11

[24] Dee, D.P., Uppala, S.M., Simmons, A.J., Berrisford, P., Poli, P., Kobayashi, S., Andrae, U., Balmaseda, M.A., Balsamo, G., Bauer, P., Bechtold, P., Beljaars, A.C.M., Berg, L., Bidlot, J., Bormann, N., Delsol, C., Dragani, R., Fuentes, M., Geer, A.J., Haimberger, L., Healy, S.B., Hersbach, H., Hólm, E.V., Isaksen, L., Kållberg, P., Köhler, M., Matricardi, M., McNally, A.P., Monge-Sanz, B.M., Morcrette, J.-J., Park, B.-K., Peubey, C., Rosnay, P., Tavolato, C., Thépaut, J.-N., Vitart, F.: The ERA-Interim reanalysis: configuration and performance of the data assimilation system. Quarterly Journal of the Royal Meteorological Society **137**(656), 553–597 (2011) https://doi.org/10.1002/qj.828 . Accessed 2019-05-03

[25] Waters, J., Lea, D.J., Martin, M.J., Mirouze, I., Weaver, A., While, J.: Implementing a variational data assimilation system in an operational 1/4 degree global ocean model. Quarterly Journal of the Royal Meteorological Society **141**(687), 333–349 (2015) https://doi.org/10.1002/qj.2388 . _eprint: https://rmets.onlinelibrary.wiley.com/doi/pdf/10.1002/qj.2388. Accessed 2025-07-21

[26] Good, S.A., Martin, M.J., Rayner, N.A.: EN4: Quality controlled ocean temperature and salinity profiles and monthly objective analyses with uncertainty estimates. Journal of Geophysical Research: Oceans **118**(12), 6704–6716 (2013) https:

//doi.org/10.1002/2013JC009067 . _eprint: https://onlinelibrary.wiley.com/-doi/pdf/10.1002/2013JC009067. Accessed 2024-10-11

[27] Reynolds, R.W., Smith, T.M., Liu, C., Chelton, D.B., Casey, K.S., Schlax, M.G.: Daily High-Resolution-Blended Analyses for Sea Surface Temperature. Journal of Climate **20**(22), 5473–5496 (2007) https://doi.org/10.1175/2007JCLI1824.1 . Publisher: American Meteorological Society Section: Journal of Climate. Accessed 2024-10-11

[28] Zweng, M.M., Reagan, J.R., Antonov, J.I., Locarnini, R.A., Mishonov, A.V., Boyer, T.P., Garcia, H.E., Baranova, O.K., Johnson, D.R., Seidov, D., Biddle, M.M.: World ocean atlas 2013. Volume 2, Salinity (2013) https://doi.org/10.7289/V5251G4D . Publisher: U.S. Department of Commerce, National Oceanic and Atmospheric Administration, National Environmental Satellite, Data and Information Service. Accessed 2025-07-08

[29] Meier, W.N., Stewart, J.S.: Assessing uncertainties in sea ice extent climate indicators. Environmental Research Letters **14**(3), 035005 (2019) https://doi.org/10.1088/1748-9326/aaf52c . Publisher: IOP Publishing. Accessed 2024-07-22

[30] Meier, W.N., Peng, G., Scott, D.J., Savoie, M.H.: Verification of a new NOAA/NSIDC passive microwave sea-ice concentration climate record. Polar Research (2014) https://doi.org/10.3402/polar.v33.21004 . Accessed 2024-10-08

[31] Cavalieri, D.J., Gloersen, P., Campbell, W.J.: Determination of sea ice parameters with the NIMBUS 7 SMMR. Journal of Geophysical Research: Atmospheres **89**(D4), 5355–5369 (1984) https://doi.org/10.1029/JD089iD04p05355 . _eprint: https://onlinelibrary.wiley.com/doi/pdf/10.1029/JD089iD04p05355. Accessed 2024-12-12

[32] Comiso, J.: Bootstrap Sea Ice Concentrations from Nimbus-7 SMMR and DMSP SSM/I-SSMIS. (NSIDC-0079, Version 4). NASA National Snow and Ice Data Center Distributed Active Archive Center., Boulder, Colorado USA. (2023). https://doi.org/10.5067/X5LG68MH013O

[33] Meier, W.N., Fetterer, F., Windnagel, A.K., Stewart, J.S.: NOAA/NSIDC Climate Data Record of Passive Microwave Sea Ice Concentration. National Snow and Ice Data Center., Boulder, Colorado USA (2021). https://doi.org/10.7265/efmz-2t65

[34] Facility, E.O.a.S.I.S.A.: Global sea ice concentration climate data record 1978-2020 (v3.0, 2022), OSI-450-a, https://cds.climate.copernicus.eu/cdsapp#!/dataset/satellite-sea-ice-concentration

[35] Cavalieri, D.J., Crawford, J.P., Drinkwater, M.R., Eppler, D.T., Farmer, L.D., Jentz, R.R., Wackerman, C.C.: Aircraft active and passive microwave validation of sea ice concentration from the Defense Meteorological Satellite Program special sensor microwave imager. Journal of Geophysical Research: Oceans **96**(C12), 21989–22008 (1991) https://doi.org/10.1029/91JC02335 . _eprint: https://agupubs.onlinelibrary.wiley.com/doi/pdf/10.1029/91JC02335. Accessed 2025-10-06

[36] Murphy, A.H., Daan, H.: Forecast Evaluation. In: Probability, Statistics, And Decision Making In The Atmospheric Sciences. CRC Press, ??? (1985). Num Pages: 59

[37] Libera, S., Hobbs, W., Klocker, A., Meyer, A., Matear, R.: Ocean-Sea Ice Processes and Their Role in Multi-Month Predictability of Antarctic Sea Ice. Geophysical Research Letters **49**(8), 2021–097047 (2022) https://doi.org/10.1029/2021GL097047 . _eprint: https://agupubs.onlinelibrary.wiley.com/doi/pdf/10.1029/2021GL097047. Accessed 2025-07-30

[38] Roach, L.A., Dörr, J., Holmes, C.R., Massonnet, F., Blockley, E.W., Notz, D., Rackow, T., Raphael, M.N., O'Farrell, S.P., Bailey, D.A., Bitz, C.M.: Antarctic Sea Ice Area in CMIP6. Geophysical Research Letters **47**(9), 2019–086729 (2020) https://doi.org/10.1029/2019GL086729 . _eprint: https://onlinelibrary.wiley.com/-doi/pdf/10.1029/2019GL086729. Accessed 2025-04-28

[39] Bunzel, F., Notz, D., Baehr, J., Müller, W.A., Fröhlich, K.: Seasonal climate forecasts significantly affected by observational uncertainty of Arctic sea ice concentration. Geophysical Research Letters **43**(2), 852–859 (2016) https://doi.org/10.1002/2015GL066928 . _eprint: https://onlinelibrary.wiley.com/-doi/pdf/10.1002/2015GL066928. Accessed 2024-08-16

Supplementary figures

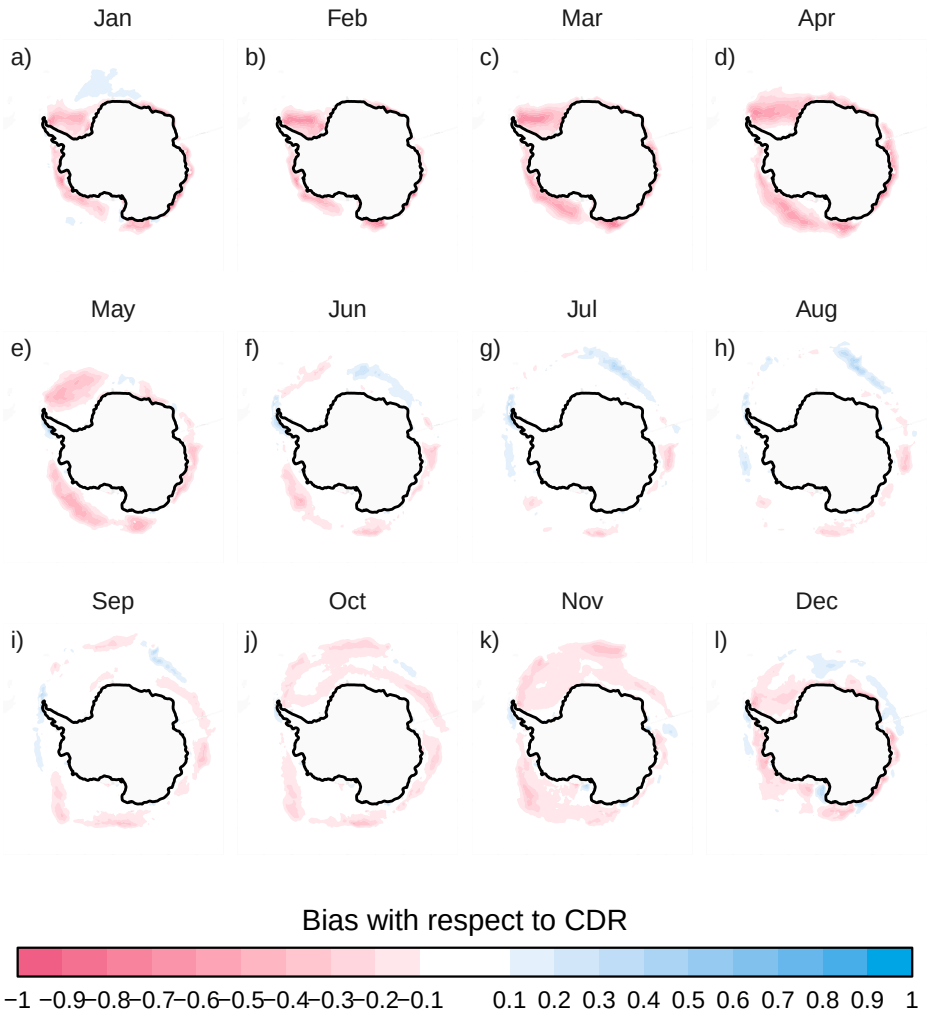

Figure 3: Ensemble mean difference between monthly sea-ice concentration of ACCESS-S2 ensemble mean forecast at 0-month lead time (monthly mean values forecasted from the forecast initialised at the first of the month) and observations.

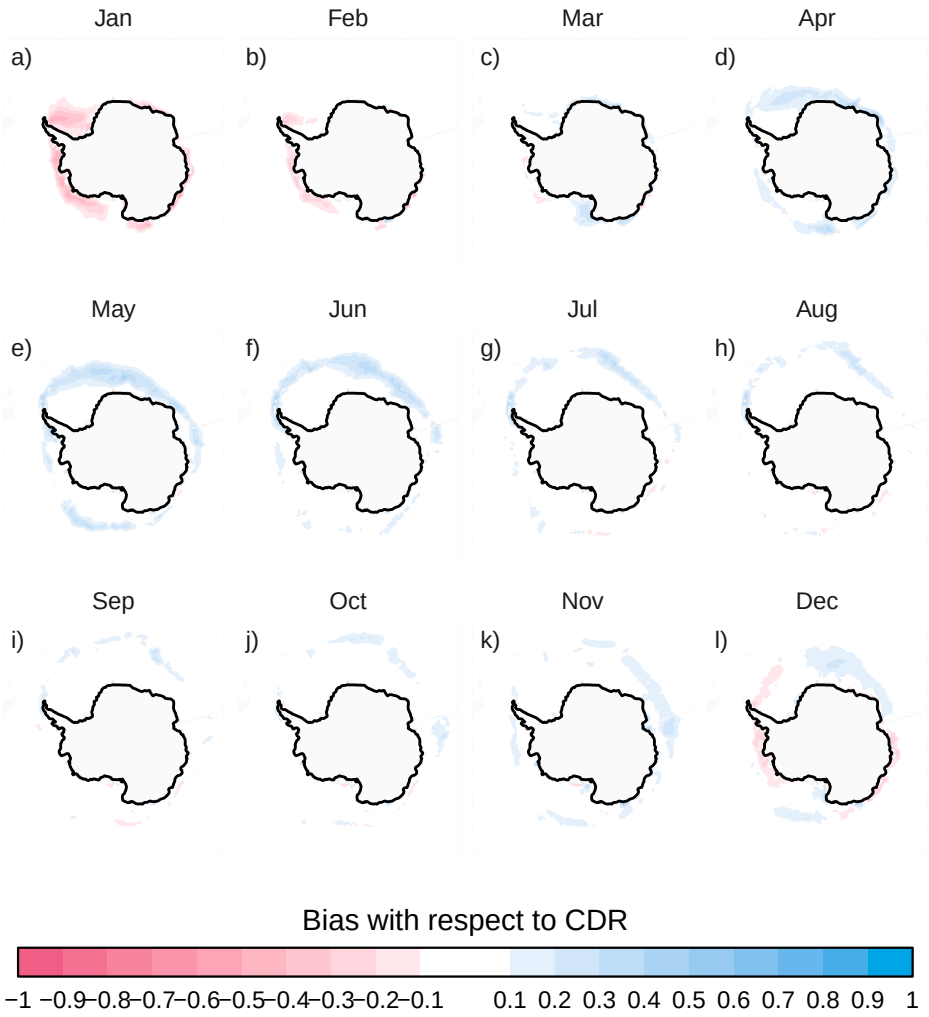

Figure 4: Same as Figure 3 but for ACCESS-S1

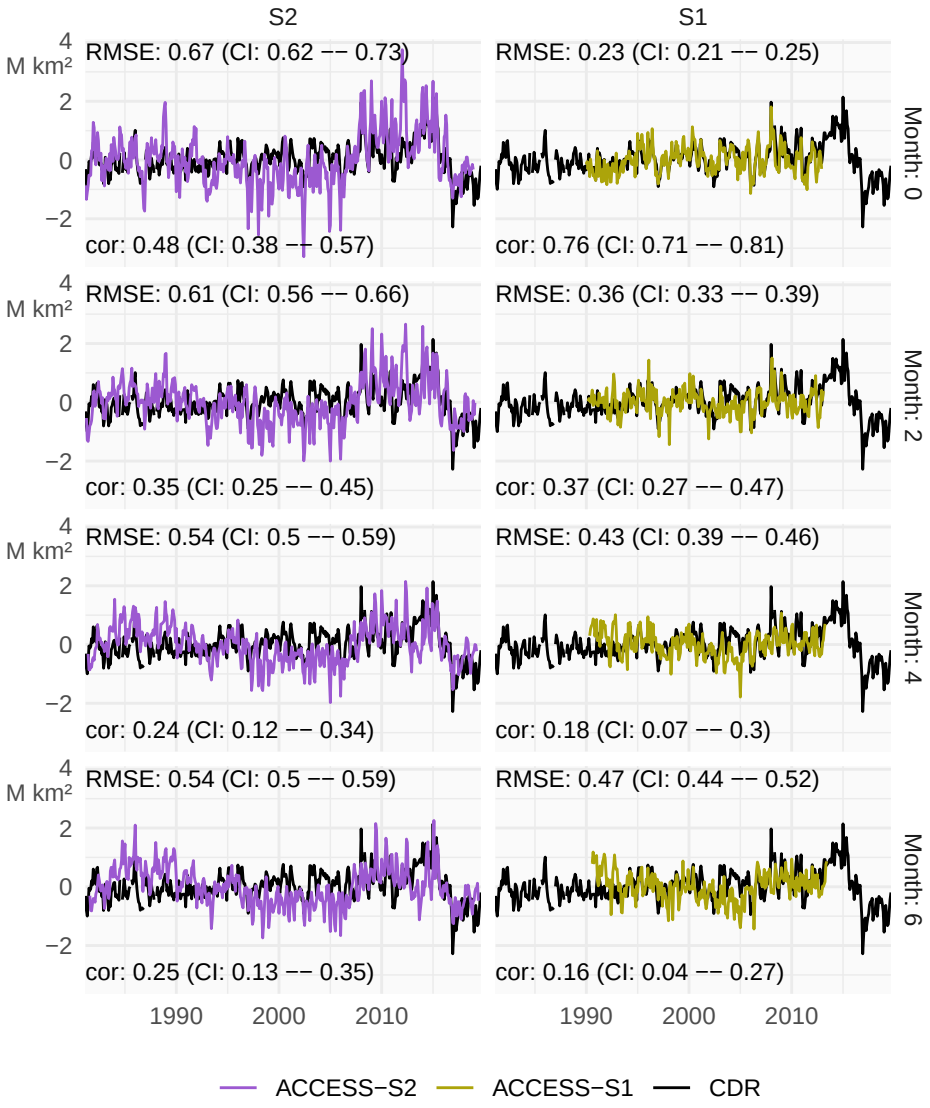

Figure 5: Monthly mean sea-ice extent anomalies of the observations (black) and forecasts from ACCESS-S1 (right column; purple) and ACCESS-S2 (left column; green) at lead times of 0, 2, 4, and 6 months. The RMSE and correlation during the overlapping period of ACCESS-S1 and ACCESS-S2 hindcasts (1990–2013) is shown on the top left and bottom left of each panel respectively.

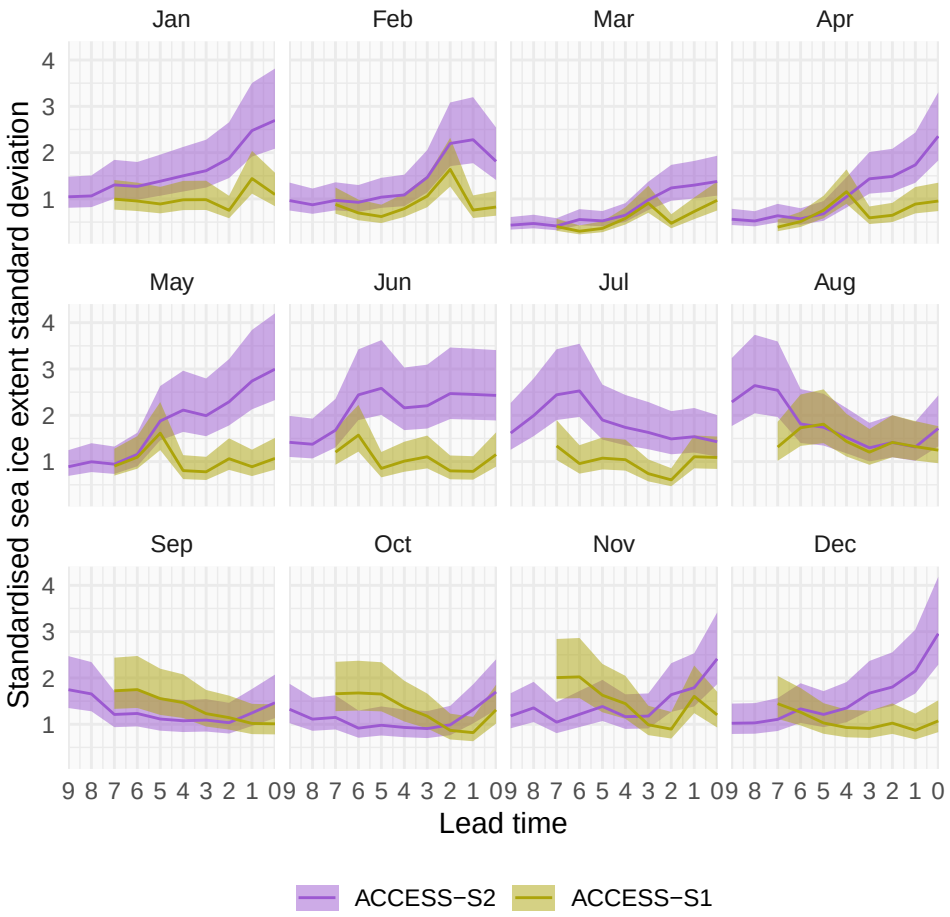

Figure 6: Interannual standard deviation with 95% confidence interval of monthly mean sea-ice extent forecasted for each month divided by that month's sea-ice extent observation standard deviation. ACCESS-S1 and ACCESS-S2 at different lead times. Each panel indicates the target month. Note the reverse horizontal axis.

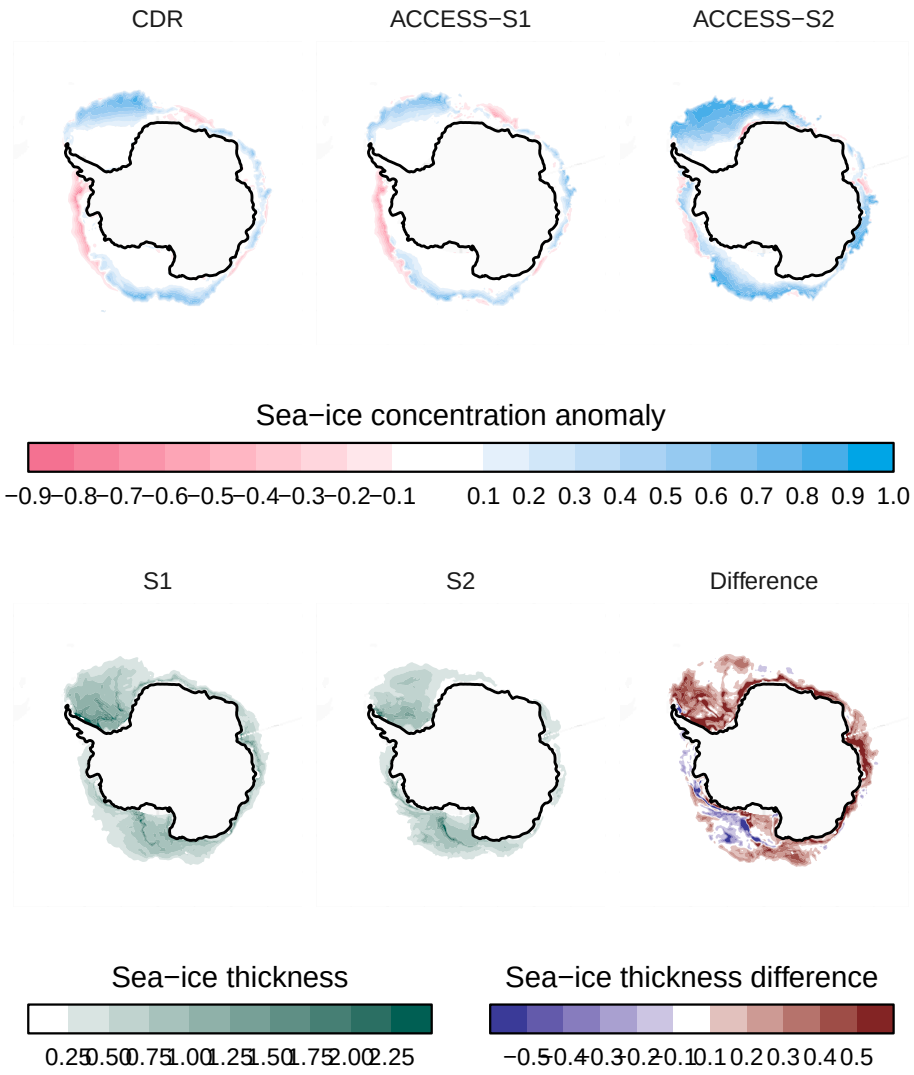

Figure 7: ACCESS-S1 and ACCESS-S2 hindcasts for 2 May 2008 at one day lead time. Top row shows sea-ice concentration anomalies forecasted by each system and the observations. Bottom row shows forecasted sea-ice thickness and the difference between ACCESS-S1 and ACCESS-S2.

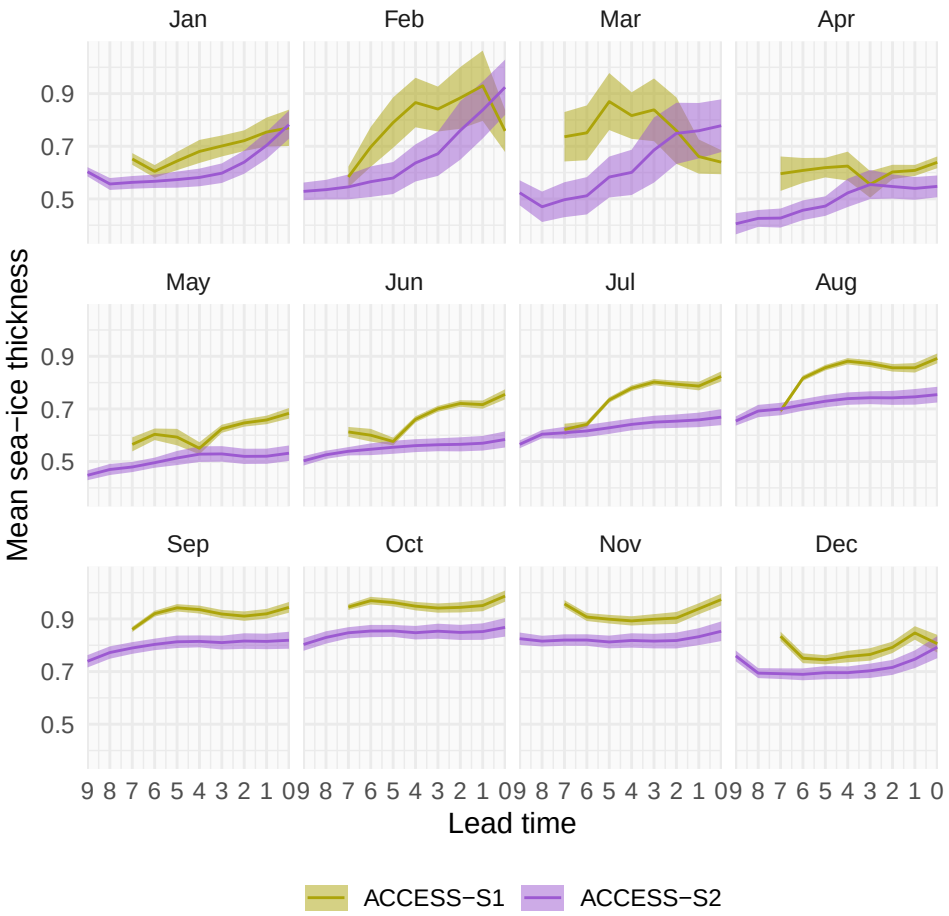

Figure 8: Mean and 95% interval of monthly mean sea-ice thickness for ACCESS-S1 and ACCESS-S2 at different lead times. Each panel indicates the target month. Note the reverse horizontal axis.

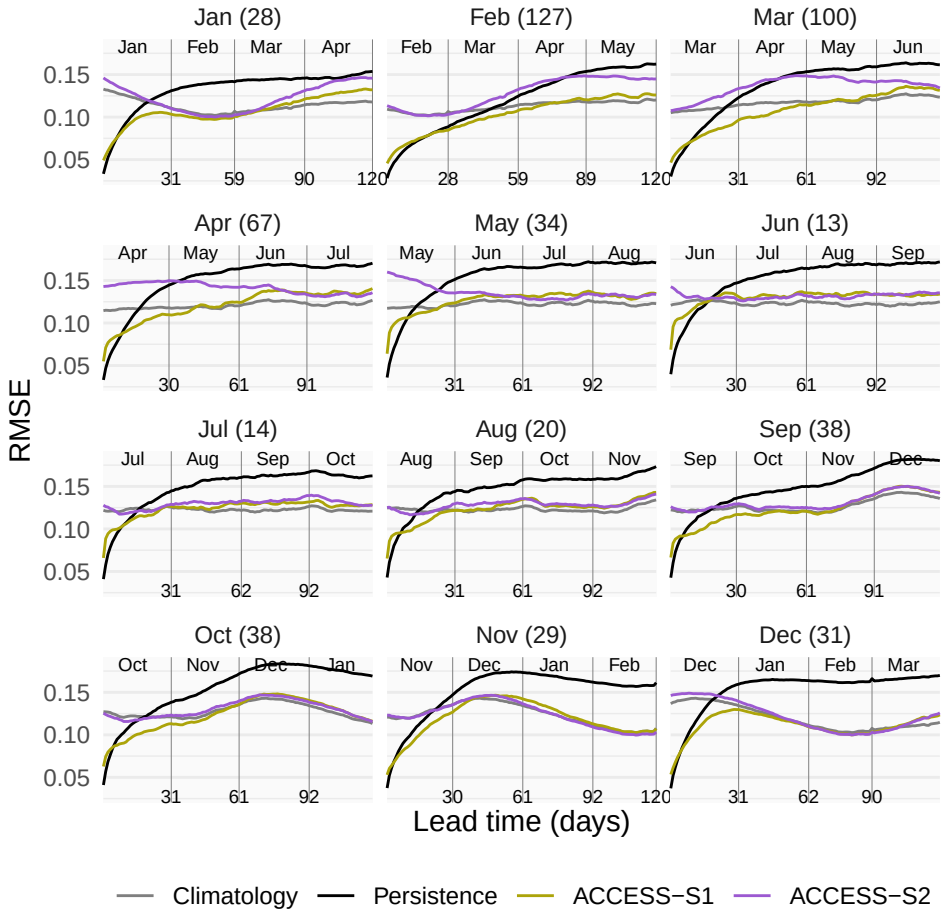

Figure 9: Mean RMSE of sea-ice concentration anomalies as a function of forecast lead time for all forecasts initialised on the first of each month compared with a reference forecast of persistence of anomalies (black) and climatology (gray). Only the first 120 days are shown. In parenthersis, the shortest time at which ACCESS-S1 and ACCESS-S2 mean RMSE is not statistically different at the 99% confidence level.

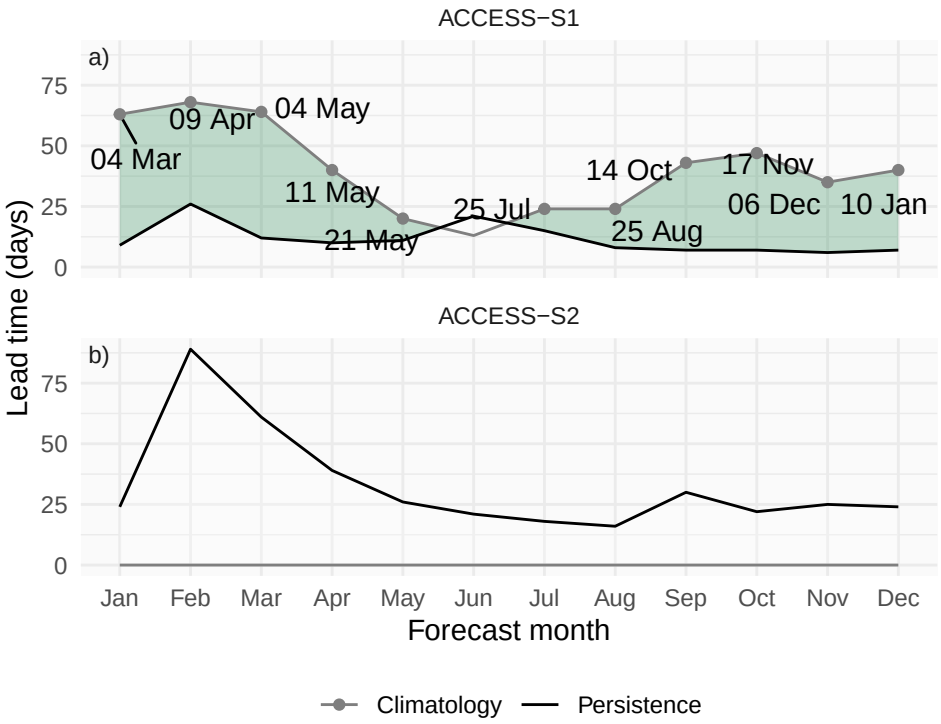

Figure 10: Minimum lead time at which each forecast's mean RMSE becomes larger than the lower bound of the 95% confidence interval of persistence forecast RMSE (black lines) and maximum lead time at which each forecast's mean RMSE remains lower than the lower bound of the 95% confidence interval of climatological forecast RMSE (gray lines). Green shading indicates the window where forecasts outperform both persistence (lead times longer than black line) and climatology (lead times shorter than gray line). Text labels show the date corresponding to the maximum lead time at which each forecast outperforms climatology.

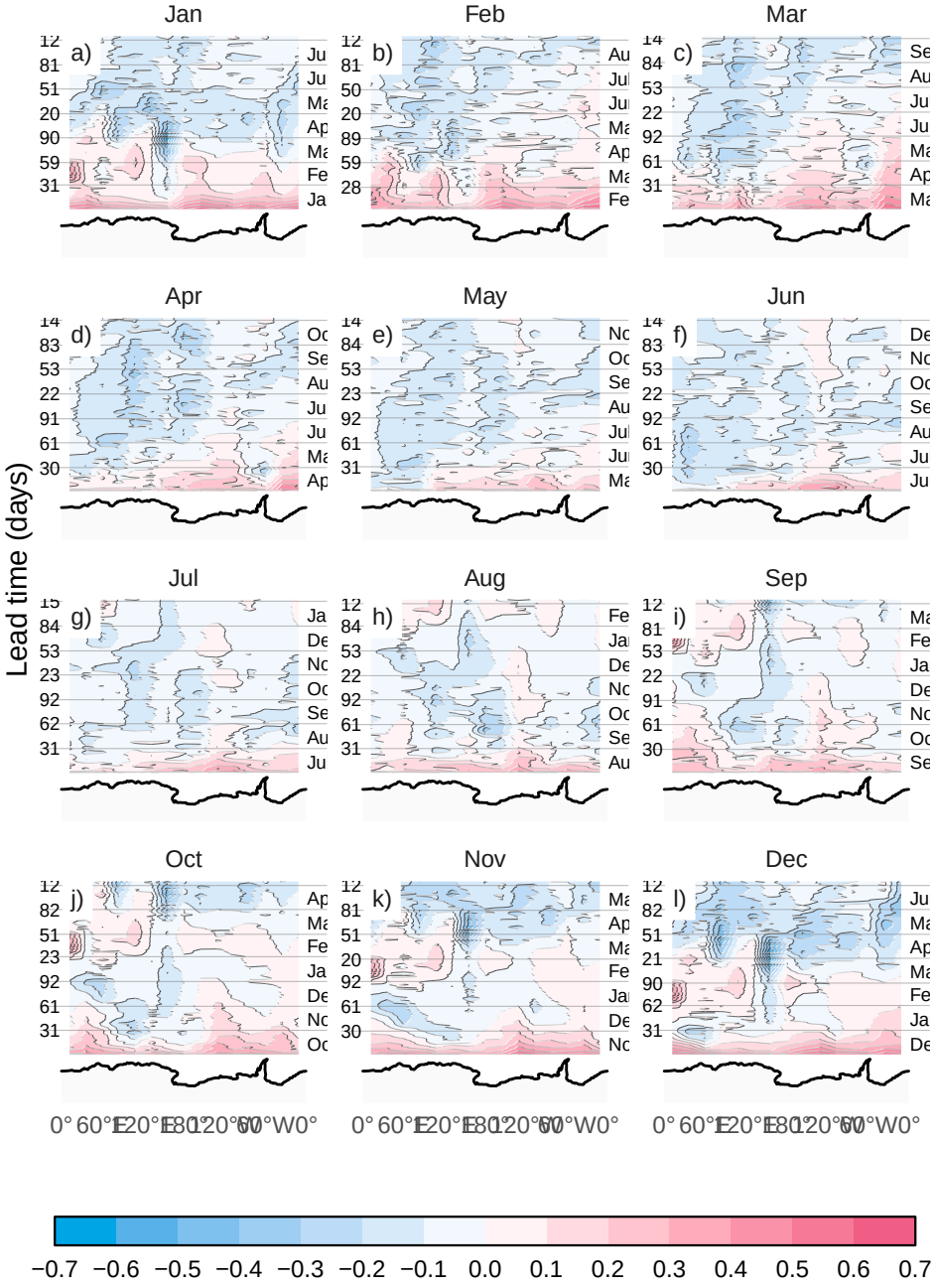

Figure 11: RMSE skill score of ACCESS-S1 forecasts with climatological forecast as reference computed on 15 meridional slices 24º wide as a function of lead time and longitude. Antarctica's coastline is shown at the bottom of each panel for reference.

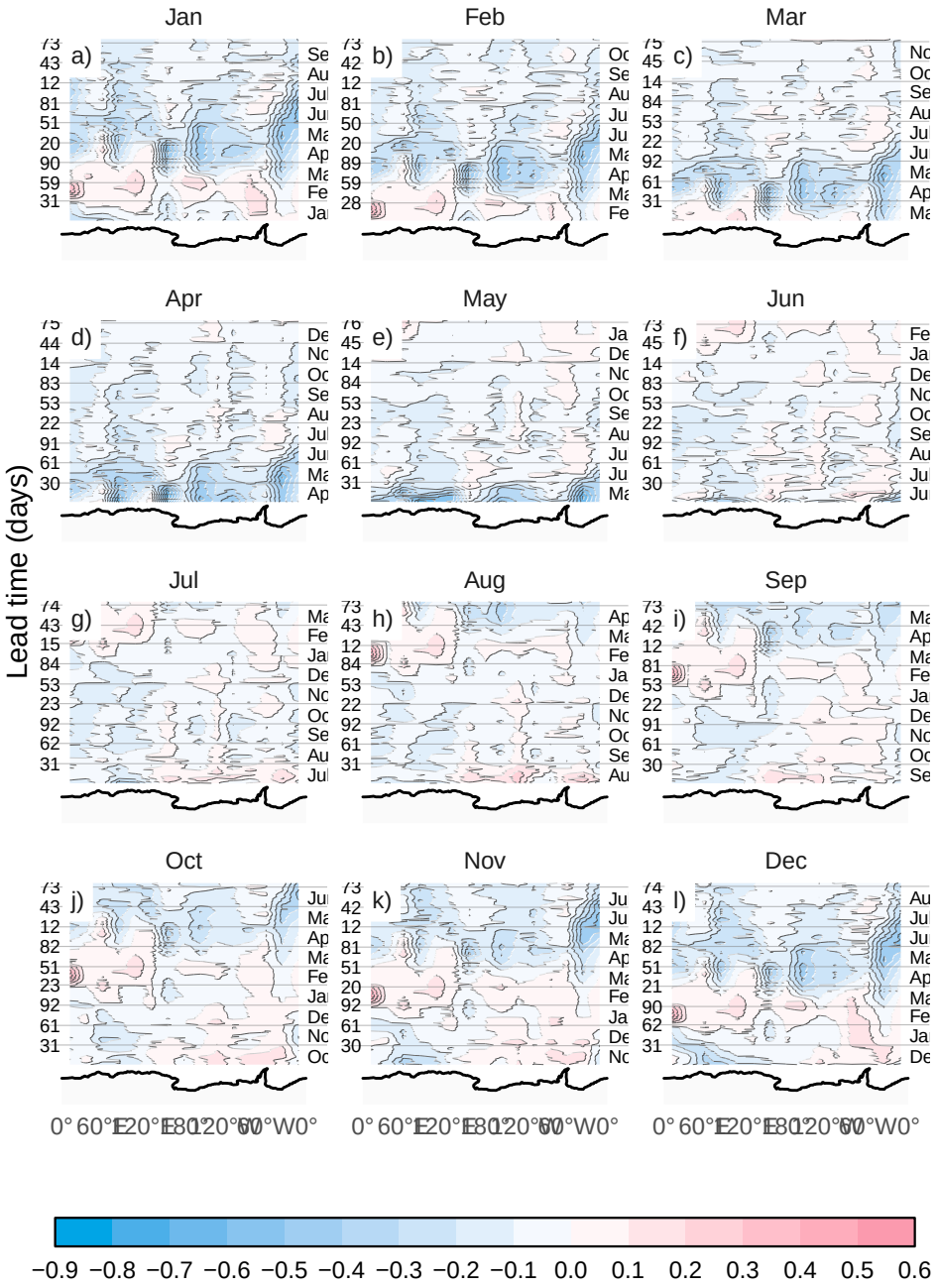

Figure 12: Same as Figure 11 but for ACCESS-S2

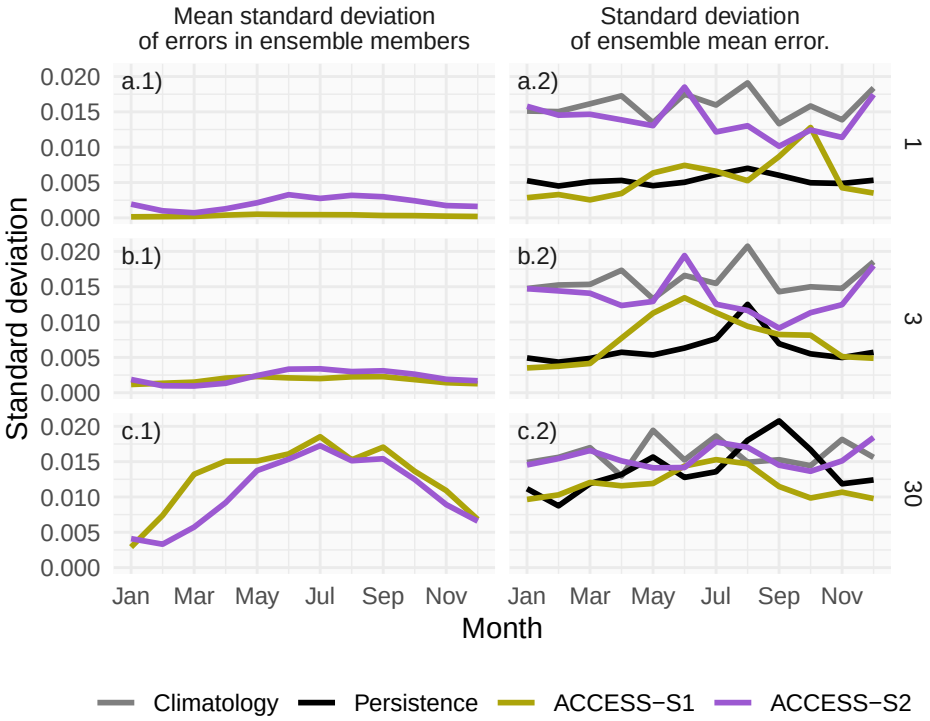

Figure 13: Decomposition of forecast error spread at 1, 5 and 30 days lead time for ACCESS-S1 and ACCESS-S2 hindcasts across initialization months. The left column shows the mean standard deviation of RMSE errors across ensemble members, while the right column shows the standard deviation of the ensemble mean RMSE error and the spread of the persistence and climatology forecasts errors.